

# Helicopter Rotor Dynamics Optimization with Experimental Verification

Mark W. Davis\* and William H. Weller†

United Technologies Research Center, East Hartford, Connecticut 06108

An automated design optimization analysis was developed to efficiently predict helicopter blade structural properties leading to improved dynamic behavior. Modal-based optimization criteria were defined for calculation by a coupled-mode eigenvalue analysis. The optimization analysis was applied to various rotor dynamics problems to predict potential design benefits and evaluate techniques for improving optimizer performance. Design parameter scaling, algorithm selection, and objective function formulation were shown to have a significant influence on optimizer performance. Two experimental programs were also conducted to verify the analysis. In each program, formal optimization techniques were applied to modify the structural properties of dynamically scaled models to improve certain operating characteristics. In the first, the edgewise structural bending-stiffness distribution of a bearingless rotor model flexure was optimized to maximize the edgewise structural damping ratio, while maintaining acceptable blade frequency placement. In the second, the blade spanwise mass distribution and structural bending stiffness of an articulated rotor model were varied to minimize rotor vibratory loads in forward flight. Direct comparison of experimental results from baseline and optimized rotors for each test program verified the reliability of the selected optimization criteria and showed that the modal-based analysis can be used to achieve significant improvements in aeromechanical stability and rotor vibratory response.

## Nomenclature

$dm$	= mass per infinitesimal blade cross section, lb-s <sup>2</sup> /in.
$e$	= hub flapping hinge spanwise offset, in.
$F_i$	= generalized forcing function for $i$ th blade mode, lb
$g$	= gravitational acceleration, in./s <sup>2</sup>
$g_i$	= $i$ th inequality constraint function
$h_j$	= $j$ th equality constraint function
$I_i$	= generalized inertia for $i$ th blade mode, lb-s <sup>2</sup> /in.
$J$	= scalar objective function
$K$	= edgewise stiffness of shear-restraint damper for bearingless rotor, lb/in.
$P$	= natural frequency normalized by rotor speed (per rev)
$S_{ij}$	= $j$ th component of modal shear or moment of $i$ th blade mode, lb/in.
$T$	= rotor thrust, lb
$T_{1g}$	= nominal thrust for 1g flight, lb
$\bar{X}$	= vector of design variables
$x_k$	= $k$ th design variable
$x_k^l, x_k^u$	= lower and upper bounds on $k$ th design variable, respectively
$\beta$	= pseudodesign variable used in Min $\beta$ problem formulation
$\beta_i$	= $i$ th pseudodesign variable used in Min $\Sigma\beta$ problem formulation
$\delta_i$	= shear-restraint damper edgewise deflection for $i$ th blade mode, in./in.
$\zeta_i$	= equivalent viscous damping ratio for $i$ th blade mode
$\theta_0$	= rotor collective pitch angle at 75% radius, deg
$\mu$	= advance ratio (normalized wind-tunnel airspeed)
$\phi$	= elastomeric material loss angle for shear-restraint damper, rad
$\phi_{ij}$	= $j$ th component of mode shape for $i$ th blade mode, in./in. or rad

$\Omega$	= rotor rotational speed, rpm
$\omega$	= forcing function frequency in vibration index, rad/s
$\omega_i$	= natural frequency of $i$ th blade mode, rad/s
$\omega_{i_{opt}}$	= target frequency for $i$ th natural frequency, $\omega_i$ , rad/s

## Introduction

IN the last two decades, optimization methodology has become a powerful tool in expediting mechanical design. Its utility stems from 1) the elimination of costly man-in-the-loop iterations, 2) the potential for novel or superior designs which might not otherwise be realized within practical constraints of time and cost, and 3) the ability to efficiently integrate multidisciplinary criteria earlier in the design process. Whereas these techniques have been applied to a fairly wide range of aeronautical engineering problems,<sup>1</sup> the helicopter industry has only recently begun to exploit their capabilities.<sup>2</sup> One reason is that the comprehensive aeroelastic analyses required to completely model the complex aerodynamic environment and the transmission of dynamic loads from the rotor to the fuselage are still too computationally expensive and unproven to fully support the design of a new helicopter. As a result, helicopter design process tends to follow an evolutionary path with new designs evolving from previous designs with a significant amount of engineering experience and trial and error required.

As helicopter applications, flight envelopes, and mission requirements have grown, the need for significant improvements in operational attributes has become more urgent and has motivated the helicopter industry to strive for more revolutionary designs. To develop new commercial markets, improved performance efficiency, higher cruise speeds, reduced noise for urban flying, and a "jet-smooth ride" throughout the operating envelope must be provided. New machines and missions envisioned for the military, such as LHX, will require maneuvering capabilities well beyond those of the current inventory and, thus, will require significant design improvements. In meeting these increased requirements, automated optimization techniques will be necessary to simultaneously consider the many design parameters, multidisciplinary criteria, and their interactions present in the

Received Oct. 11, 1989; revision received April 19, 1990; accepted for publication April 19, 1990. Copyright © 1989 by the American Institute of Aeronautics and Astronautics, Inc. All rights reserved.

\*Research Engineer, Rotorcraft Dynamics Group.

†Supervisor, Rotorcraft Dynamics Group.

design process. References 3–11 represent some of the recent efforts in applying optimization techniques to rotor dynamic problems. Only Refs. 7 and 11 present test results to support analytical predictions. There is a clear need for validation of analytically predicted results before the industry can make further progress in developing optimization criteria and analyses for use in the actual design process.

The work presented herein summarizes research conducted at United Technologies Research Center (UTRC) in helicopter rotor dynamics optimization. Four areas have been emphasized: 1) development of a modal-based rotor blade optimization analysis, BLDOPT, that is sufficiently efficient and accurate for use in design studies, 2) development of modal-based optimization criteria that reliably yield significant improvements in rotor dynamic response, 3) development of experimental facilities suitable for directly comparing the dynamic characteristics of baseline and optimum designs, and 4) verification of the BLDOPT analysis and optimization criteria by performing experimental tests. BLDOPT, documented in Ref. 8, is an automated analysis that optimizes blade modal characteristics through tailoring of structural properties. Although prediction of blade dynamic response requires an aeroelastic analysis, studies based on modal characteristics are important for several reasons. First, existing aeroelastic analyses are not sufficiently accurate to reliably predict designs with improved characteristics on a consistent basis. Second, it has been demonstrated in Ref. 11 that significant improvements in rotor dynamic properties can be made through refinements reflected in blade modal characteristics. Finally, studies based on modal analyses can be carried out much more efficiently than with aeroelastic analyses. The large run times associated with closed-loop aeroelastic optimization are illustrated by Ref. 10. Although such run times are acceptable to the researcher, they are totally unacceptable for production codes. Thus, it is more likely that modal-based optimization analyses will be incorporated into the preliminary design process as long as they accurately project significant improvements in rotor design.

In the first half of this paper, results based on the analytical studies of Ref. 8 are presented to demonstrate the effect of parameter scaling, algorithm selection, and objective function formulation on the efficiency and reliability of achieving an optimum solution. In the second half, results are presented for two experimental programs conducted to demonstrate the capability of BLDOPT to predict blade structural properties leading to improved helicopter dynamic behavior. In each program, formal optimization techniques were applied to modify the structural properties of dynamically scaled model rotor designs to optimize certain operating characteristics. Modal-based optimization criteria were calculated by an eigenvalue analysis. In the first program, the edgewise structural damping ratio for a bearingless rotor model was maximized to achieve greater aeromechanical stability margins. In the second program, selected vibration criteria were minimized to reduce rotor vibratory loads in forward flight. Direct comparison of experimental results from baseline and optimized rotors are presented for each program to substantiate the modal-based optimization criteria and to verify analytically predicted improvements in rotor aeromechanical stability and vibratory response.

### Design Optimization Methodology

To apply numerical optimization techniques to the helicopter design process, problems are posed mathematically as follows

Minimize:

$$J(\bar{X}) \quad (1)$$

Subject to:

$$g_i(\bar{X}) \leq 0 \quad i = 1, L \quad (2)$$

$$h_j(\bar{X}) = 0 \quad j = 1, M \quad (3)$$

$$x_k^l \leq x_k \leq x_k^u \quad k = 1, N \quad (4)$$

where design vector  $\bar{X} = [x_1, \dots, x_N]$  and scalar  $J$  is the objective function to be minimized. The inequality constraint functions,  $g_i(\bar{X})$  and equality constraint functions  $h_j(\bar{X})$  represent design criteria that must be satisfied for the design to be feasible or acceptable. Side constraints  $x_k^l$  and  $x_k^u$  are, respectively, lower and upper bounds placed on the  $k$ th design variable. The feasible design space includes all designs that satisfy the constraints represented by Eqs. (2–4). The “optimum” design corresponds to the minimum value of the objective function that occurs in the feasible design space. Most state-of-the-art optimization algorithms can be thought of as an iterative process of calculating a search direction in the design space, minimizing the objective function in this direction, and checking for convergence. The results presented herein are based on first-order algorithms, which use gradient information, with perhaps some approximation to the Hessian matrix to determine the search direction.

### Closed-Loop Optimization Analysis

A closed-loop analysis, BLDOPT, has been developed to optimize blade dynamic behavior through structural tailoring of blade properties. BLDOPT is comprised of an optimization program, a blade eigenvalue program, and an executive controlling program developed to link the former two programs.

### General-Purpose Optimization Program

The Automated Design Synthesis (ADS) program<sup>12,13</sup> is incorporated into the closed-loop analysis as a general-purpose optimization program having a wide selection of algorithms for solving constrained or unconstrained minimization problems. The program is organized into three basic levels: strategy, optimizer, and one-dimensional search. Several options available at each level give the user significant flexibility to select an algorithm best suited to a given design problem.

### Blade Eigenvalue Program

The system analysis, BLDMODE, is a coupled-mode eigenvalue computer program based on the analysis of Ref. 14. The program computes blade modal characteristics (e.g., natural frequencies and mode shapes) based on the Holzer-Myklestad formulation adapted for rotating beams. The Ref. 14 analysis was modified to improve program efficiency and accuracy and to expand its modeling capabilities, including the capability to analyze bearingless rotors with pitch horn or shear-restraint control systems. In addition to traditional modal parameters (e.g., blade natural frequencies), several other parameters are calculated by BLDMODE for use in design optimization studies. As described in a following section, each of these parameters is defined to yield information pertinent to rotor dynamic behavior.

### Executive Controlling Program

The executive controlling program links the ADS optimization and BLDMODE eigenvalue programs into a closed-loop blade design optimization analysis and provides the structure for formulating the optimization problem. The user is given considerable flexibility in formulating the objective function and selecting design variables and constraint functions. The user can select almost any BLDMODE structural input parameter as a design variable. Several strategies are also available for linking various groups of structural parameters to one or more design variables. Finally, most modal parameters calculated for each blade mode (e.g., blade natural frequency, blade-root shear, and vibration index) and certain structural parameters can be selected as either components of the objective function or as constraint functions.

### Optimization Algorithms Evaluated

Analytical studies were performed to evaluate the efficiency and reliability of seven optimization algorithms from three classes. Their characteristics are described briefly presently. Detailed discussions can be found in Refs. 15–18.

#### Indirect Penalty Methods

Indirect penalty methods transform the constrained optimization problem into an unconstrained subproblem by defining a pseudo-objective function that combines the true objective function with a weighted penalty term for constraints. Typically, the value of the scalar weighting factor greatly affects the solution to the unconstrained subproblem. Values that ensure near satisfaction of all constraints usually result in highly nonlinear, ill-conditioned problems that may not be solvable from the initial design. Therefore, the scalar value is varied as the optimum solution is approached through a sequence of unconstrained subproblems. Many such algorithms exist, which are characterized by the form of the penalty function used and the scheme for updating the scalar multiplier. Three representative algorithms are evaluated: exterior penalty (Ext. Pen.), extended interior penalty (Int. Pen.), and augmented Lagrange multiplier (ALM). Regardless of which indirect penalty method is used, each subproblem must be solved by an unconstrained optimization algorithm. The Broydon-Fletcher-Goldfarb-Shanno (BFGS) variable metric method<sup>16,17</sup> is used for all indirect penalty method results presented herein.

#### Approximate Methods

Approximate methods solve a sequence of subproblems that involve some approximation to the design space. Two algorithms are studied. The first is sequential linear programming (SLP), which solves a sequence of subproblems involving explicit linear approximations to all objective and constraint functions. Once the approximate subproblem is generated from gradient information, it can be readily solved using either linear programming techniques or the direct methods discussed below. The second algorithm considered here is sequential quadratic programming (SQP),<sup>16,17</sup> which incorporates second-order information into the process by solving a quadratic subproblem to determine the search direction. This subproblem involves minimizing a quadratic approximation to the objective function augmented by the Lagrangian function, while satisfying linear approximations to the constraint functions. An unconstrained one-dimensional search is then performed using the full system analysis and augmenting the true objective function with Lagrange multipliers and an exterior penalty in a manner similar to the ALM algorithm. At each step in the SQP sequence, calculated gradients are used to refine the quadratic approximation with prescribed update formulas.

#### Direct Methods

Direct methods deal explicitly with both nonlinearities and constraints. Two algorithms are evaluated. Both are gradient-based feasible direction methods that generally follow the constraints to the optimum, while maintaining a feasible design. The first is the method of feasible directions (MFD),<sup>17</sup> which determines the search direction by solving a subproblem involving the gradients of the objective function and all active constraints. The resulting search direction lies generally along but not tangential to the active constraint boundaries to ensure that the objective function is initially reduced and active constraints are not immediately re-encountered. The second approach is the modified method of feasible directions (MMFD).<sup>18</sup> For MMFD, the MFD direction-finding subproblem is modified to account directly for equality constraints and to proceed tangentially along the more critical active constraints.

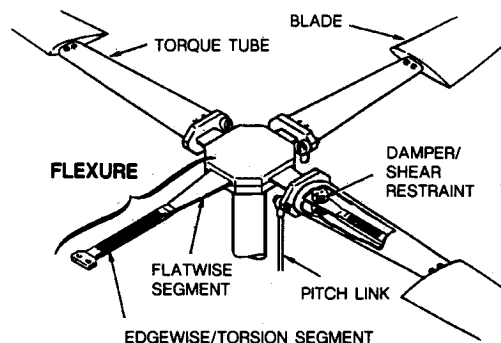


Fig. 1 Bearingless main rotor design concept.

### Applications to Helicopter Dynamics Problems

#### Bearingless Rotor Aeromechanical Stability

An example of state-of-the-art in helicopter main rotor designs is the soft-in-plane bearingless rotor configuration, illustrated by Fig. 1. The bearingless rotor is characterized by structural flexures that connect each blade's aerodynamic section to the hub center. The flexures are designed to accommodate bending motion in the flatwise (out-of-plane), edgewise (in-plane), and torsion (pitch) directions. For the configuration illustrated in Fig. 1, the flexure is enclosed by a torsionally stiff torque tube used to transfer pitch control inputs to the blade aerodynamic section by twisting the outboard portion of the flexure. The flexure, torque tube, and blade are bolted together at the outboard end of the flexure. At the inboard end of the torque tube, a shear-restraint mechanism connects the torque tube to the flexure. By restricting flatwise motions of the torque tube, flatwise-torsion coupling and flexure loads that would result from pitch link shears are minimized. For the edgewise restraint, elastomeric shear pads are used to tailor the load distributions in the different parts of the structure and to augment structural damping in the edgewise direction. A dual load path is present in the spanwise region between the shear-restraint station and the outboard juncture of the flexure, torque tube, and blade. The design of each part must be tailored to optimize the sharing of loads between the two paths.

One of the chief issues in designing bearingless rotors is aeromechanical stability. The problem involves coupling between the edgewise motions of the rotor blades and motions of the fuselage at the hub. This is an issue during the rotor startup sequence when the fuselage pitches or rolls about its landing gear while setting on the ground or during autorotation when rotor speed is also varied from its nominal flight value. When a rotor blade moves in the edgewise direction, its center of gravity is displaced in the plane of the rotor relative to the center of rotation, imposing a centrifugal force that alternately acts on the fuselage in both pitch and roll directions. When the edgewise motions of the blades occur at their fundamental natural frequency, a whirl mode is established. The whirl mode frequency varies with rotor speed, and rotor speeds within the operating range often lead to a coalescence of the whirl and lower-frequency fuselage modes. For soft-in-plane bearingless rotor systems, where the edgewise frequency is less than the rotor speed, this coalescence may create an aeromechanical instability. Reference 19 shows that the potential for an instability of this type can be eliminated by adding sufficient amounts of structural damping to affect edgewise motions of the blade. Thus, the shear-restraint mechanism of the bearingless rotor must provide a level of damping suitable for the prevention of aeromechanical instabilities. As discussed in Ref. 19, the contribution of the shear-restraint damper to the rotor's mode damping ratio is given by the expression

$$\zeta_1 = \frac{K \cdot \delta_1^2 \cdot \tan(\phi)}{2 \cdot I_1 \cdot \omega_1^2} \quad (5)$$

where  $K$  represents the edgewise stiffness of the shear-restraint damper and  $\tan(\phi)$  is the damper material loss tangent. The terms  $\delta_1$ ,  $I_1$ , and  $\omega_1$  are the damper modal deflection, generalized inertia, and natural frequency for the fundamental edgewise mode. As shown in Ref. 19, the damping arising from the shear-restraint damper forms the greatest part of the total for the isolated rotor at up to 1g thrust conditions. Therefore, this formulation is used to quantify the bearingless rotor's edgewise damping characteristics in design studies.

#### Low-Vibration Rotor Design

One of the most detrimental characteristics of helicopter operations is the imposition of vibrations on the airframe from the loads incurred on the rotor blade in flight. The reduction of rotorcraft vibratory response has been a constant challenge to the helicopter industry. Analysis of the complex structure and operational environment of the helicopter requires the use of state-of-the-art aeroelastic predictive programs that are too computationally expensive and, perhaps, unproven to be employed early in the design process. Thus, preliminary rotor blade dynamic design has traditionally been based on the simplistic criteria of placing natural frequencies to avoid resonances with harmonics of the rotor's rotational speed. Although this criteria guards against the more excessive levels of blade and hub vibratory loads, it does not guarantee that minimum, or even acceptable, vibration levels will occur. Mechanical isolation and attenuation devices are also employed to further reduce vibration levels in the airframe to desired levels. However, these devices result in increased weight and maintenance costs with decreased reliability. With the more stringent vibration and reliability requirements of future rotorcraft, vibration levels must be further reduced and with less complex approaches. The rotor must be made inherently less responsive through improved design.

Several modal-based properties are used in assessing the inherent blade dynamic characteristics pertinent to vibration. In addition to the natural frequency associated with each mode, two other terms, based on the equations of Ref. 20, are also used to characterize vibration attributes: the modal shear and vibration index. The modal shear of the  $i$ th mode is defined by the relationship

$$S_{ij} = \omega_i^2 \int \phi_{ij} \cdot dm \quad (6)$$

where  $\omega_i$  is the natural frequency,  $\phi_{ij}$  is the mode shape component which determines the  $j$ th shear type (i.e., vertical or horizontal), and  $dm$  is a mass element along the span. The  $S_{ij}$  term is the cumulative inertial reaction force per unit tip deflection at the blade root due to vibration of the mode. A more complete description of the vibration characteristics of a blade is given by the vibration index expression

$$\text{Vibration index} = \frac{[\omega_i^2 \int \phi_{ij} \cdot dm] F_i}{\omega_i^2 \cdot I_i \sqrt{[1 - (\omega/\omega_i)^2]^2 + [2 \zeta_i (\omega/\omega_i)]^2}} \quad (7)$$

where  $I_i$  is the generalized inertia,  $\zeta_i$  is the modal damping ratio,  $F_i$  is the generalized forcing function, and  $\omega$  is the frequency of the forcing function. All of the terms included in this expression, except  $F_i$ , are standard modal parameters. The forcing function  $F_i$  was derived empirically to allow calculation within the eigenvalue analysis. Since the vibration index not only contains the modal shear term, but also the forcing function, generalized inertia, and damped amplification, it should be a more reliable indicator of the vibration characteristics of a rotor blade.

### Illustration of Design Optimization Procedures

#### Sample Design Optimization Problems

The analysis BLDOPT was applied to solve four representative problems to evaluate the effectiveness of al-

ternative optimization algorithms, problem formulations, and solution strategies. Only an overview is presented here, but more detailed results from the analytical study can be found in Ref. 8. The techniques presented here are similar to those used to achieve the optimized designs tested and presented in the section entitled "Experimental Verification of Optimized Rotor Designs." The examples selected illustrate a range of problem complexity, as exemplified by the number and type of components considered in the design objective. For the stability problem, only a single term is required, whereas for the vibration problems, between four and 15 components are considered. Therefore, the tendency to encounter local minima in the design space due to tradeoffs between components varies for each problem.

#### Bearingless Rotor Aeromechanical Stability

Ten design variables, including the shear-restraint edgewise spring rate and edgewise bending stiffness of the torque tube and eight hub flexure segments, are used. The objective is to maximize the bearingless rotor damping ratio, defined in Eq. (5), of the fundamental edgewise mode while maintaining bounds of 0.69 to 0.71P (per rev) on the modal frequency. Design parameter ranges are restricted to between 75 and 200% of initial values to provide a sufficiently large but viable design space to project potential design benefits. This example is a fairly simple optimization problem having a single-component objective function as well as relatively few design variables and constraints. Since ADS is formulated to solve minimization problems, the negative of the damping ratio is minimized to achieve a maximum in its actual value.

#### Low-Vibration Rotor Design

The remaining three problems focus on reducing vibratory response on a four-bladed, articulated rotor. The first of these is concerned with simultaneously placing frequencies of one horizontal and three vertical modes. The other two problems involve minimizing the magnitude of the modal shears or vibration indices, according to Eq. (6) or (7), for three of these same modes. Thirty-three design variables, composed of the blade weight, beamwise bending stiffness, and chordwise bending stiffness at 11 spanwise blade segments, are used for these problems. Design parameter ranges are restricted to between 75 and 200% of the initial blade design values. Constraints of  $\pm 5\%$  on total blade weight and flapping inertia are also imposed. Two characteristics must be addressed in formulating these problems. First, each problem involves multiple objectives. Second, each criterion is associated with a component to be minimized in magnitude or zeroed rather than minimized in the classic sense. To address these concerns, a sum-of-the-squares formulation for the objective function is used, except where noted. Although this formulation is later shown to be effective, it does complicate the optimization process by increasing the nonlinearities present in the design space.

For the frequency placement problem, the blade design is modified to move the second vertical mode frequency from 2.76 to 2.5P, the third vertical from 4.8 to 4.5P, the fourth vertical from 7.7 to 8.5P, and the second horizontal from 4.6 to 5.5P. For this problem, each component of the objective function is composed of the square of the difference between one frequency and its target value. For the minimized modal shear problem, both horizontal and vertical shears for three critical modes (i.e., second and third vertical and second horizontal) are minimized. Therefore, six modal parameter values are included in the objective function. Unlike the frequency placement problem, however, it is unlikely that a null objective function can be practically achieved. For the fourth problem, the modal vibration indices for the same three critical modes used in the shear problem are considered. Five indices for each mode (i.e., 3P and 5P horizontal shear, 4P vertical shear, and 3P and 5P hub moment) are included in the objective function, resulting in fifteen components to be

minimized. Each vibration index is composed of four non-linear functions, including both modal frequency and blade shear, and it is unlikely that all 15 indices can be zeroed simultaneously. Due to the number and complexity of objective function components, there is significant potential for local minima in this problem.

#### Parameter Scaling

Both the structural damping and frequency placement problems were solved with the MMFD algorithm and different parameter scaling strategies to determine the effect on optimizer performance (e.g., satisfaction of optimization criteria and efficiency). Four different scaling approaches were evaluated: no scaling, normalization only, ADS scaling only, and normalization with ADS scaling. With no scaling, design variable, constraint function, and objective function values are provided to the optimizer in the same engineering units used within the system analysis, BLDMODE. Normalization involves dividing each variable by its initial absolute value to ensure that the solution process is not dominated by the relative magnitude of any one parameter. The ADS scaling uses a sophisticated strategy to scale all parameters to ensure that no function dominates due to the magnitude of its gradient components.<sup>13</sup> The last approach involves ADS scaling of normalized variables.

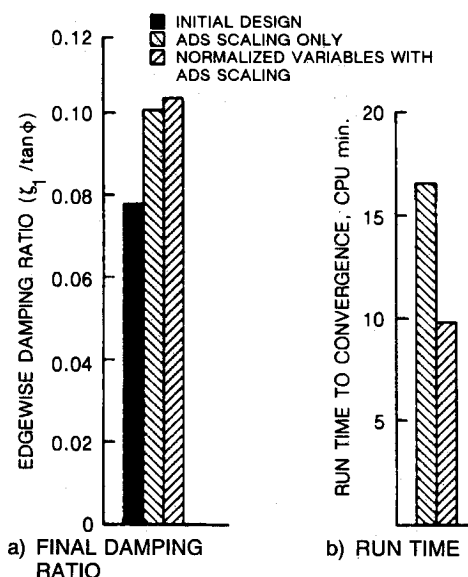


Fig. 2 Effect of variable normalization on optimizer performance for maximizing bearingless rotor structural damping.

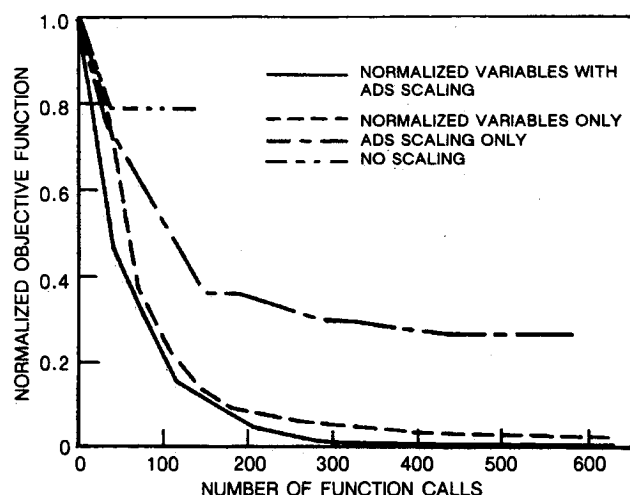


Fig. 3 Comparison of normalization and scaling effects on optimizer performance for placing rotor blade frequencies.

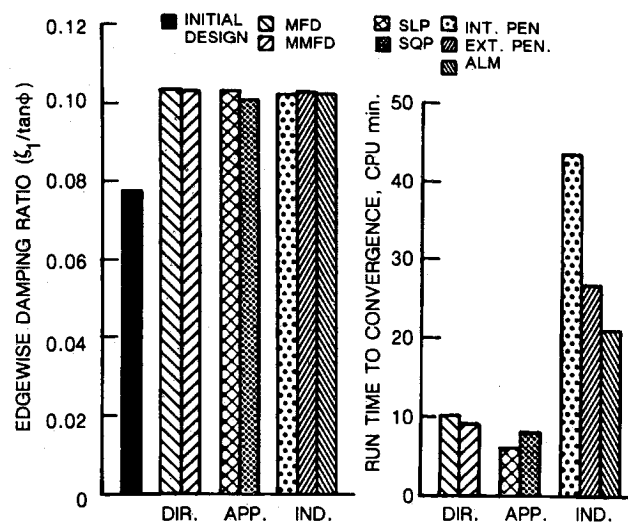


Fig. 4 Effect of algorithm selection on optimizer performance for maximizing bearingless rotor structural damping.

Figure 2 compares the performance of the MMFD algorithm when solving the edgewise structural damping problem using either ADS scaling only or normalization with ADS scaling. BLDOPT was very effective with both approaches, achieving a 30% increase in the damping ratio over that of a conventional baseline design, while maintaining the blade frequency of the first edgewise mode within tightly prescribed limits. However, the use of normalized variables improved the performance of the MMFD algorithm significantly even for this relatively simple problem. Use of normalized variables achieved an additional 4% increase in the damping ratio in 40% less time. Note that all run times cited in this paper are based on Perkin-Elmer 3200 series computer processing units (CPU) of time.

Figure 3 compares the performance history of the MMFD algorithm when implementing all four scaling approaches to solve the frequency placement problem. The objective function, normalized by its initial value, is plotted against the number of function calls to the system analysis, including calls required to calculate gradients via finite differences. On each curve, the straight line segments connect normalized objective function values at the end of each iteration. Note that a zero value of the objective function represents exact satisfaction of all four frequency targets. Optimizer performance was best when using both normalization and ADS scaling. Scaling by normalization only was almost as effective. On the other hand, the optimizer was not effective when using ADS scaling only or with no scaling. Due to the significant difference in magnitude between nonscaled values of blade mass and bending-stiffness parameters, the optimizer without normalization focused on mass variations almost exclusively and could not satisfy all four target frequencies simultaneously. Although more sophisticated scaling strategies can be devised, simple normalization is highly effective and should generally be implemented. The ADS scaling approach could not overcome the problem of large differences in variable magnitudes but did fine-tune optimizer performance when using normalized variables. Both parameter normalization and ADS scaling were used to achieve all remaining results.

#### Algorithm Selection and Effectiveness

All four sample problems were solved with the seven algorithms described earlier to evaluate relative performance. All solutions were achieved by starting each algorithm from the same initial design and using normalized variables with ADS scaling. Figure 4 compares the performance of all seven algorithms for the structural damping problem. All were equally effective, resulting in similar design solutions, al-

**Table 1 Equivalent objective function and run time required by alternative algorithms and objective function formulations**

	ABS	Sum Sq.	Sum with Bound	Min $\beta$	Min $\Sigma\beta$
MFD	0.21 — <sup>a</sup>	0 <sup>b</sup> (1:20)	0.03 (0:49)	0.01 (0:43)	0 (1:32)
MMFD	0.29 —	0 (0:34)	0.02 (0:53)	0.01 (0:58)	0 (1:28)
SLP	0.56 —	0.43 —	0 (0:31)	0 (0:53)	0 (1:08)
SQP	0 (0:26)	0 (0:27)	0 (0:32)	0 (0:57)	0 (0:29)
Int. Pen.	0.24 —	0 (3:01)	0.23 —	0 (3:03)	0.08 —
Ext. Pen.	0.18 —	0 (6:51)	0.25 —	0 (4:00)	0 (5:00)
ALM	0.23 —	0 (5:58)	0.05(14:29)	0 (6:46)	0 (10:49)

<sup>a</sup>A dash denotes that a 95% reduction was not achieved.

<sup>b</sup>A single zero (0) denotes values less than 0.005.

though the computational time required varied dramatically. Both direct (DIR.) and approximate (APP.) methods were quite efficient in solving the problem with approximate methods providing the fastest convergence. The indirect (IND.) methods required much more time due to their solving a sequence of optimization problems based on the full system analysis. Further, the Exterior Penalty and ALM methods allowed constraint violations early in the design process before increasing the penalties to ensure a feasible design at convergence. Stopping these two algorithms prematurely to prevent excessive run times could have resulted in infeasible designs. The SLP algorithm also did not guarantee continually improving designs due to the approximate nature of the linearized subproblem at each iteration.

For the frequency placement problem, all algorithms, except SLP, were equally effective in providing solutions that satisfied all four frequency targets. The SLP algorithm was unable to satisfy more than two frequency targets in this example. Again, there was a significant difference in the computational requirements for each algorithm. The MMFD and the SQP algorithms were the two most efficient, requiring less than 34 CPU min to achieve a 95% reduction in the quadratic objective function. The computational requirements of the indirect penalty methods exceeded 3 CPU h for all three algorithms.

Figure 5 compares the effectiveness of the MMFD, SQP, and ALM algorithms in solving the blade-root shear problem. Each of these represents the generally best performing algorithm in its class, as determined by the studies reported here and in Ref. 8. In Fig. 5, the final values of the predicted vertical and horizontal shears for each of the three critical modes are compared to initial values. All three algorithms were equally effective in minimizing the quadratic six-component objective function and achieved similar solutions. Over 40% reductions were obtained in all predicted shears

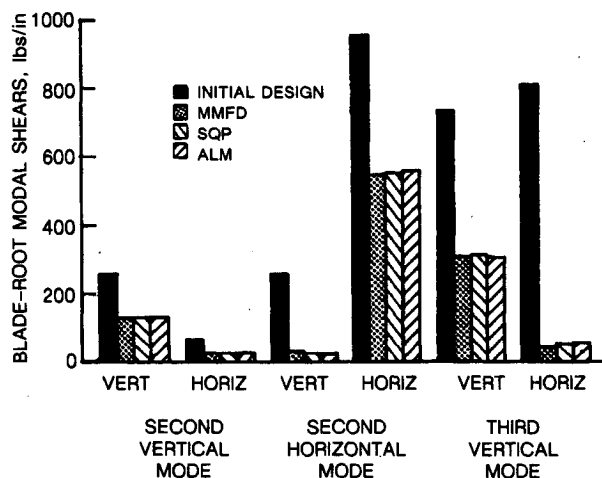


**Fig. 5 Effect of algorithm selection on optimizer performance for minimizing modal shears.**

with significantly larger reductions in some. Convergence times required by MMFD, SQP, and ALM were 1:57, 1:18, and 3:11 CPU h, respectively.

Figure 6 compares the effectiveness of the same three algorithms in reducing the indices included in the objective function for the vibration index problem. Note that only the nine most pertinent indices, having the largest initial values, are shown for clarity. All 15 indices were reduced by all three algorithms, including seven by over 40%. These results correspond to at least a 70% reduction in the quadratic 15-component objective function. The designs reached by the three algorithms were similar in many respects, although some significant differences were apparent. In addition to being slightly more effective in reducing the objective function, SQP required 40% less time to converge than both MMFD and ALM. Convergence times required by MMFD, SQP, and ALM were 3:27, 2:00, 3:26 CPU h, respectively. These results are atypical, however, in that MMFD was usually much more efficient than ALM in reaching optimum solutions.

#### Objective Function Formulation

Five alternative objective function formulations were studied to determine their effect on optimizer performance in solving the low-vibration rotor problems having multiple objective criteria. Only results for the frequency placement and vibration index problems are presented here. Additional results can be found in Ref. 8. The first formulation (ABS) is composed of a sum of the absolute values of the differences between each parameter and its target value. The second (Sum Sq) is the quadratic sum-of-the-squares formulation discussed earlier. The third formulation (Sum with Bounds) places each parameter directly into the objective function with an appropriate sign to either minimize or maximize it toward a

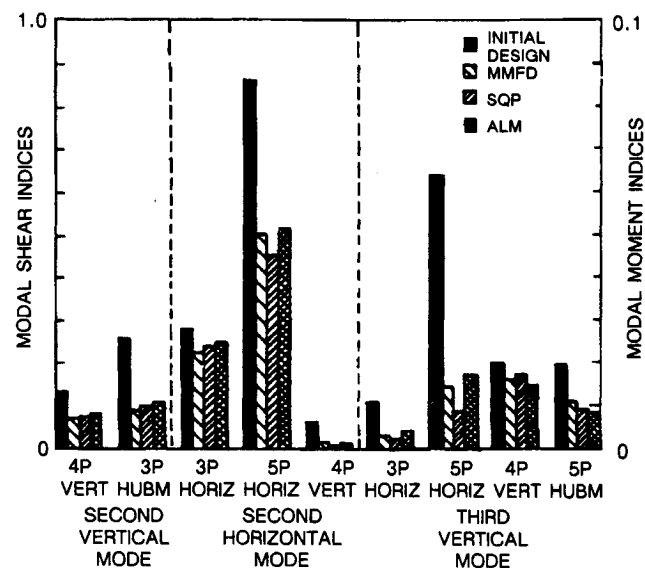


**Fig. 6 Effect of algorithm selection on optimizer performance for minimizing modal vibration indices.**

constraint bound placed at its target value. This formulation results in a multicomponent objective function comprised of continuous terms without introducing additional nonlinearities, but eliminates part of the feasible design space. Whereas these formulations result in multicomponent objective functions, the fourth (Min  $\beta$ ) defines the objective function to be a single scalar  $\beta$ , which is also treated as an additional pseudodesign variable. Each objective criterion is then represented by a constraint set requiring the parameter to be within a  $\pm\beta$  tolerance of its target. For example, for the frequency placement problem, the Min  $\beta$  formulation requires that

$$-\beta \leq \omega_{i_{\text{opt}}} - \omega_i \leq \beta \quad i = 1, \dots, N_{\text{freq}} \quad (8)$$

where  $N_{\text{freq}}$  is the number of frequencies to be placed and  $\omega_{i_{\text{opt}}}$  is the target for the  $i$ th frequency,  $\omega_i$ . The inequalities of Eq. (8) are easily rewritten as standard constraints in the form of Eq. (2). Note that  $\beta$  cannot become negative without a violation of one of these constraints. Thus,  $\beta$  represents the instantaneous magnitude of the largest of the separations between the parameters and their respective targets. As  $\beta$  is minimized toward zero, the largest separation is reduced as well, but nothing prevents smaller separations from increasing until one of their corresponding constraints becomes active. Further, the solution process may be terminated by encountering a local minimum for one parameter. The final formulation (Min  $\Sigma\beta$ ) is similar to Min  $\beta$  but forms the objective as a sum of scalars  $\beta_i$ . Each  $\beta_i$  corresponds to one parameter, which is constrained to be within a  $\pm\beta_i$  tolerance of its target. The result is a single-component, linear objective function  $\Sigma\beta_i$ , which is a function of the pseudodesign variables  $\beta_i$  only and represents the sum of all separations. Unlike the Min  $\beta$  formulation, the inability to move one parameter closer to its target does not prevent improvements in others.

Table 1 compares the performance of all seven algorithms when solving the frequency placement problem using each of the five different objective function formulations. Table 1 shows the final equivalent objective function values calculated by using the sum-of-the-squares formulation and normalized by the initial value. It also shows in parentheses the time required to achieve a 95% reduction in the equivalent quadratic objective function.

Both Min  $\beta$  and Min  $\Sigma\beta$  proved to be viable approaches for solving problems with multiple objective criteria. However, neither formulation proved to be significantly better than Sum

Sq for this problem, except when using the SLP algorithm. Min  $\beta$  or Min  $\Sigma\beta$  may be better posed, however, for problems involving more nonlinearity and/or a larger number of objective function components as indicated by the vibration index problem that follows. Further, both Min  $\beta$  and Min  $\Sigma\beta$  formulations tended to be better behaved near the optimum than Sum Sq and converged quickly after achieving a 95% reduction in the equivalent quadratic objective function. The Sum Sq formulation had more difficulty converging due to the erratic behavior of the objective function gradient caused by nonlinearities and target crossovers near the optimum. The two remaining formulations led to generally inferior results. The ADS formulation resulted in a poorly posed problem that had a severe impact on algorithm effectiveness, due to discontinuities in calculated gradients of the objective function as the frequencies neared their targets. The Sum with Bounds formulation was not effective for several algorithms considered. With bounds placed on the frequencies, the targets could be approached from one direction only, introducing additional local minima.

SQP was generally the most effective algorithm for all problem formulations, while MMFD performed nearly as well for the three best formulations. SLP performance was problem formulation-dependent. SLP was particularly ineffective for ABS and Sum Sq, both of which increase the nonlinearity of the design space. On the other hand, SLP performed well with the remaining three formulations due to more linear objective functions and eight additional constraints, which resulted in a fully constrained problem at the optimum. The indirect methods were too inefficient to be used in general applications.

Figure 7 compares the performance of the SQP algorithm when implementing the three best performing formulations (i.e., Sum Sq, Min  $\beta$ , and Min  $\Sigma\beta$ ) to solve the vibration index problem. The Sum Sq and Min  $\Sigma\beta$  solutions had many similarities, including trends in design variables and resultant reductions in all indices. The Min  $\beta$  solution was significantly different, achieving an additional 35% reduction in the largest initial index at the expense of smaller reductions in most other indices and a slight increase in three indices. This was due to Min  $\beta$  focusing on the largest index, reducing  $\beta$  until no further reduction was possible in the 5P horizontal index of the second horizontal mode, and terminating execution without regard to further potential decreases in other components. The net result was a slightly larger reduction in the equivalent quadratic objective function when using Min  $\beta$ . For this large number of nonlinear and complex objective function components, the Min  $\beta$  and Min  $\Sigma\beta$  formulations were significantly more efficient than Sum Sq. Convergence times for Sum Sq, Min  $\beta$ , and Min  $\Sigma\beta$  were 2:00, 0:46, and 1:17 CPU h, respectively. This favorable comparison in the Min  $\beta$  and Min  $\Sigma\beta$  run times would be even better if the gradient components corresponding to the  $\beta$  or  $\beta_i$  variables were calculated analytically rather than by finite differences. It is projected that Min  $\Sigma\beta$  run times would be reduced by 20 to 30%, depending on the algorithm. The unique characteristics of the Sum Sq, Min  $\beta$ , and Min  $\Sigma\beta$  formulations make their applicability problem-dependent.

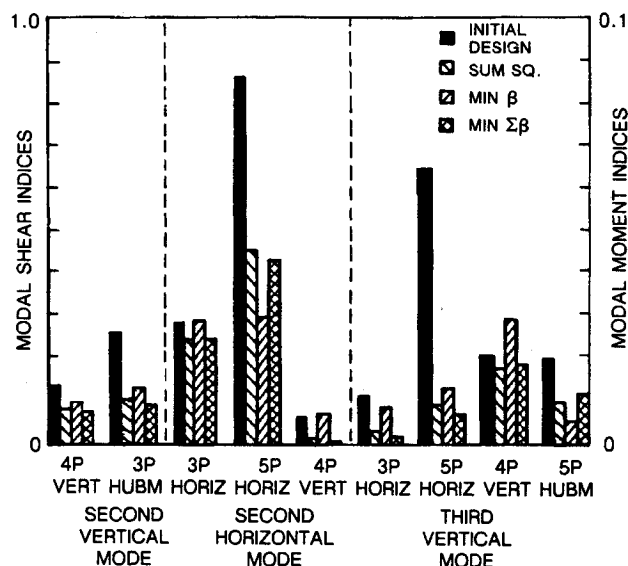


Fig. 7 Effect of problem formulation on optimizer performance for minimizing modal vibration indices.

### Experimental Verification of Optimized Rotor Designs

Two experimental programs were also conducted in conjunction with the analytical optimization studies reported in the last section. The objectives of these test programs were to verify the modal-based optimization criteria and to demonstrate the capability of the BLDOPT analysis to achieve improved helicopter dynamic behavior through blade structural tailoring. In the first program, the edgewise structural damping ratio for a bearingless rotor model was maximized to achieve improved stability margins. In the second program, selected vibration criteria were minimized to reduce vibration levels in forward flight.



### Bearingless Rotor Aeromechanical Stability

A dynamically scaled model of an early prototype rotor design had been tested in hover to yield fundamental edgewise frequency and damping trends. Analysis of the resulting data indicated that the damping levels were low and that aeromechanical instabilities were encountered at some operating conditions. An analytical optimization study was performed to identify an improved design with sufficient stability margins, while requiring minimal modifications to the existing model hardware. As an initial step, a series of sensitivity studies were performed to determine the parameters having the greatest impact on the model's stability characteristics. These studies were performed by using the optimization techniques discussed in the last section to maximize the damping ratio defined in Eq. (5) for various combinations of design variables, while maintaining initial frequency placement of the fundamental edgewise blade mode. For each set of design variables, the SQP algorithm was used to achieve a near-

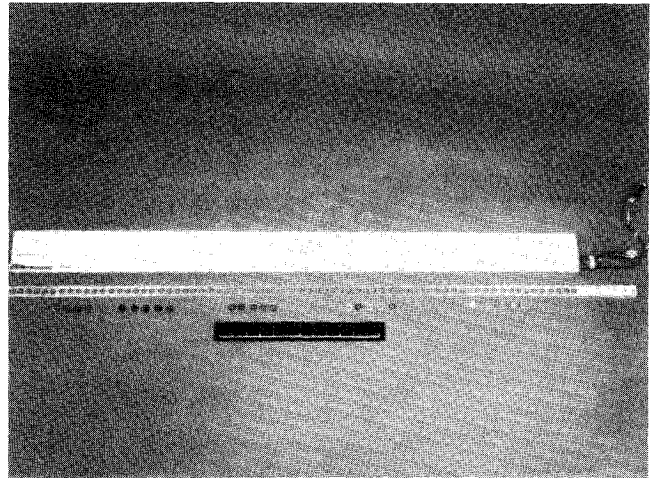


Fig. 10 Blade assembly for variable property rotor.

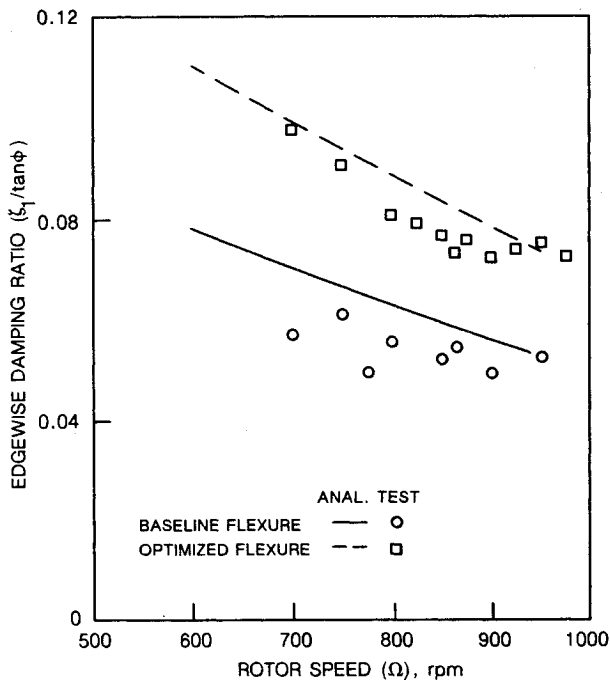


Fig. 8 Comparison of isolated rotor edgewise damping ratio for baseline and optimized flexures ( $\theta_0 = 2$  deg).

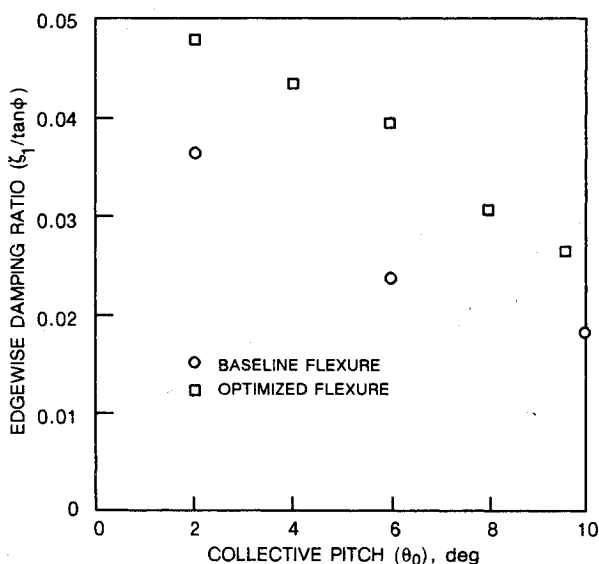


Fig. 9 Variation of edgewise damping with collective pitch at fuselage roll resonance for baseline and optimized flexures.

optimum solution because of its efficiency. Subsequently, the MFD algorithm was used to seek additional increases in damping by following the constraints to the fully constrained optimum solution. Based on these studies, it was determined that the structural damping attributed to the shear-restraint mechanism is most sensitive to the spanwise variation of edgewise bending stiffness along the flexure, the shear-restraint edgewise stiffness, the torque tube edgewise bending stiffness, and the second mass moment of inertia of the blade. The fundamental edgewise mode natural frequency is also sensitive to these same parameters. Finally, it was predicted that the rotor model's stability characteristics could be sufficiently improved just by changing the edgewise bending stiffness (i.e., planform taper) of the flexure. While changes to the other design parameters, in addition to planform changes, should further improve the stability margins, this solution was selected as being the most cost-effective to implement and verify the optimized solution.

Based on these design optimization studies, it was predicted that the structural damping of the existing rotor model could be increased by 54% by modifying the flexure edgewise taper, doubling the torque tube edgewise stiffness, increasing the shear-restraint edgewise stiffness by 47%, and increasing blade mass moment of inertia to maintain the fundamental frequency. This compares with a predicted 40% increase in structural damping arising from modification of the flexure only. The changes to the flexure's edgewise stiffness distribution were very similar for both optimized designs. In comparing the optimized and existing flexure planforms, the optimizer stiffened the inboard end and softened the outboard end with a smooth taper between. The resultant effect is a simulated hinge at the outboard end of the flexure and increased motion of the shear-restraint damper during blade edgewise bending, thereby increasing its damping contribution. It should be noted that the edgewise frequencies were 0.70 and 0.74P for the baseline and optimized rotors, respectively.

For reasons of cost, it was decided to modify only the flexure, since the damping increment associated with that solution was sufficient to assure a stable configuration. The existing model flexures were modified to achieve the design specified by the optimization studies. The modified rotor was tested at operating conditions comparable to those for the baseline model test. The effect of the modification is shown in Fig. 8, which illustrates damping trends with rotor speed at a low-collective pitch setting where the aerodynamic contribution is negligible. Both calculated structural damping and measured damping are presented for an isolated rotor (fixed-hub) condition, which served as the basis for the optimization study. Both calculated and measured damping levels are significantly increased for the optimized rotor configuration. Also, the correlation between measured



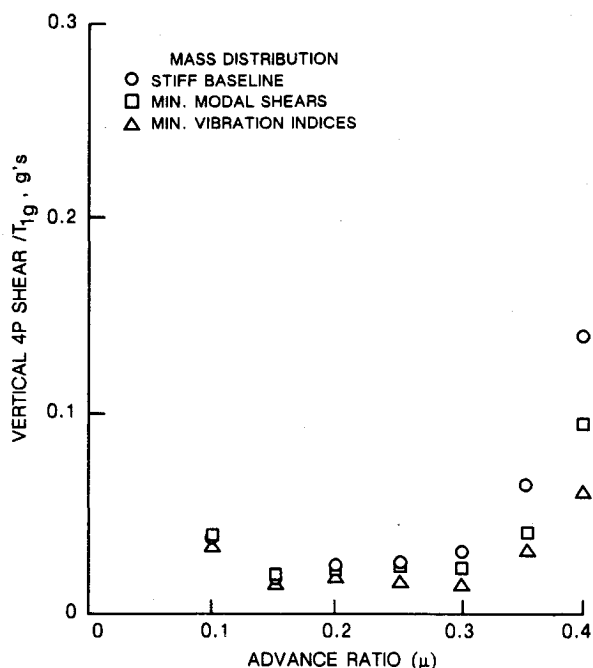


Fig. 11 Comparison of hub 4P vertical shear for minimized modal shears or vibration indices ( $T = 1g$ ).

damping and that calculated by using Eq. (5) is excellent for both original and optimized rotor models. Figure 9 illustrates the variation in damping with rotor collective pitch (thrust) for a free-hub case. These data were taken at the respective resonant rotor speeds where the rotor edgewise and fuselage roll modes coalesce. Throughout the range of collective pitch values examined, the optimized flexure led to an increase in measured system damping. Thus, the optimized flexure design, which was constrained to modifications that could be implemented on existing hardware, provided increased damping margins for operation both on the ground and in the air.

#### Low-Vibration Rotor Design

The modal shears and vibration indices, defined in Eqs. (6) and (7), have been used in a number of analytical studies at UTRC to predict blade designs having inherently low vibrations. What was lacking, however, was proof that the "optimized" designs provided the required attributes (i.e., low-vibratory loads). A test program was conducted to verify the analysis by experiment and is reviewed in Ref. 11. The program involved wind-tunnel testing of a unique rotor model having the capability to vary both the blade spanwise mass distribution and bending-stiffness values in the flatwise and edgewise directions. A picture of the rotor blade hardware is presented in Fig. 10. The mass variation was achieved by having a blade whose spar could be mechanically removed from the root end. The spar had 70 equally spaced holes along its span for installing ballast. Five different ballast weights could be inserted, providing the capability of changing weight in six equal increments at each station. The spar/ballast assembly was slipped into and mechanically fastened to a glove composed of a rectangular, hollow, composite liner bonded inside a foam airfoil section. Three sets of gloves were available with a different liner material in each to achieve the desired uniform flatwise and edgewise bending-stiffness values while maintaining identical airfoil characteristics. The blade design was such that changes in mass distribution or bending stiffness could be implemented independently. The properties of the spar, ballast weights, and glove assemblies were set to yield a variation in weight and stiffness values from 75 to 200% of the values of a nominal rotor configuration. The nominal configuration properties were, in turn, chosen to yield a model with dynamic characteristics similar to those of

a conventional full-scale rotor, using the middle stiffness blade gloves and lightest ballast weights in all 70 locations. Two other baseline configurations with the same ballast and either soft (75% nominal stiffness) or stiff (200% nominal stiffness) blade were defined. These three configurations became the starting points in optimization studies performed to define other configurations with improved vibration characteristics.

Three optimization criteria were studied: 1) placing blade natural frequencies; 2) minimizing modal shears; and 3) minimizing vibration indices. For each blade stiffness, spanwise mass distributions were defined within the range of hardware variability by minimizing the appropriate criteria. Definitions of tested configurations based on frequency placement criteria were achieved in one step. The SQP algorithm and Sum Sq formulation were used to efficiently reach an optimum solution satisfying all specified frequency targets. Unlike the frequency placement problem, it is not feasible to zero all components with practical design changes when minimizing modal shears or vibration indices. Further, frequency constraints can lead to disjointed feasible design spaces and inhibit finding a global optimum. Therefore, solutions based on these two criteria must often be obtained through a sequential process that exploits the unique characteristics of different algorithms and objective function formulations. One solution sequence used in this study is discussed here. In the first step, the BFGS unconstrained algorithm was used with a Min  $\beta$  formulation to obtain a solution reducing the largest components without regard to frequency placement to quickly determine the region of the design space containing the global optimum. The solution process was continued, using the SQP algorithm and Min  $\beta$  formulation, to obtain a solution with frequencies constrained to separations of  $0.2P$  from integer harmonics of the rotor's rotational speed. Finally, the Sum Sq formulation was used with constraints on the largest components to achieve further reductions in smaller components. In this last step, the MFD algorithm was used since this direct method has proven to be more effective near the optimum where the solution is usually fully constrained.

Tests of the baseline and optimized models were performed, using a four-bladed articulated hub, to yield data for correlating with the optimization analysis in evaluating alternative vibration reduction criteria. Figure 11 compares the

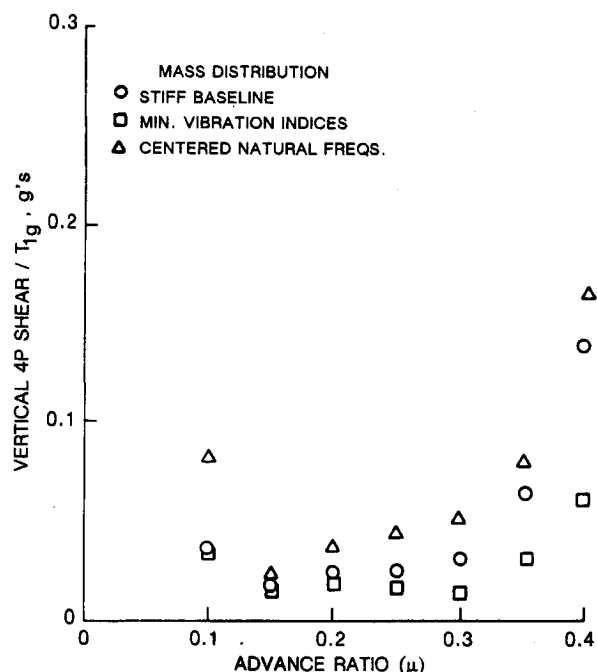


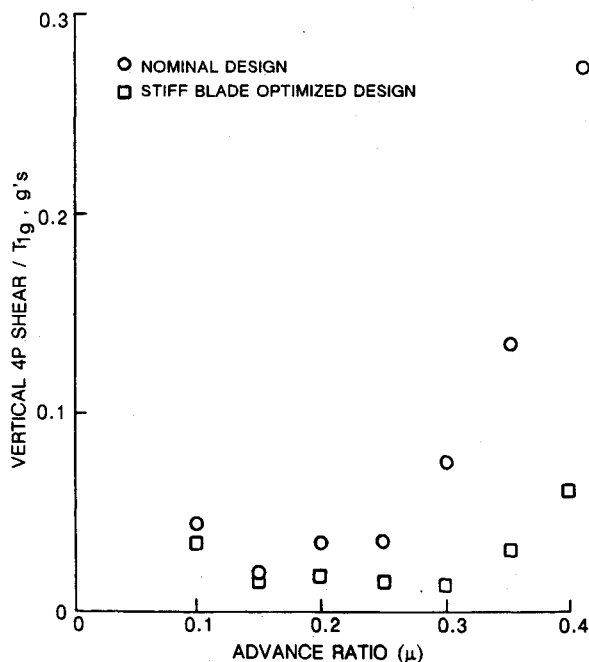
Fig. 12 Comparison of hub 4P vertical shear for two configurations with varying natural frequency placement ( $T = 1g$ ).

measured hub  $4P$  vertical vibration forces at  $1g$  thrust for the stiff baseline model with two other configurations defined by either minimizing modal shear or index values. Note that the only change between the configurations of Fig. 11 is the mass distribution. Although minimizing modal shears led to significant reductions in measured vibration levels at the higher advance ratios  $\mu$ , the design defined by minimizing vibration indices was superior in that it resulted in larger reductions in vibration levels and the reductions extended across the range tested. At the highest advance ratio, the minimum index configuration led to a 56% reduction in measured  $4P$  vertical vibration, compared to the stiff baseline rotor, while the minimized modal shear configuration was reduced by 32%. The order of the configurations with regard

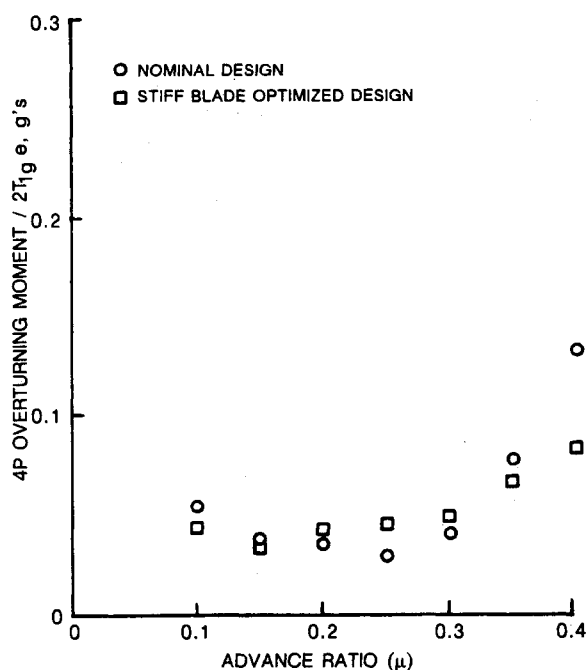
to relative measured vibration levels matched the order predicted by vibration index values calculated for all three designs. The hub  $4P$  overturning moment (hub pitch and roll moments combined), although not formally minimized, was also significantly lower for both optimized configurations. The reductions for both were comparable, verifying the analytical predictions. Results for the other two stiffness rotors were similar. Thus, the analysis consistently identified designs having lower measured vibratory response when using either the minimized modal shear or vibration index criteria with the latter providing the greatest reductions.

A demonstration of the limitations in using blade frequency placement criteria is depicted in Fig. 12, which compares the vibration characteristics at  $1g$  thrust of designs determined by using vibration index or frequency placement criteria. For the minimum index solution, a  $0.2P$  spacing between natural frequencies and harmonics of the rotor speed was maintained by constraint in the analysis. For the frequency problem, the natural frequencies for the pertinent modes were placed equidistant or centered between harmonic frequencies without regard to the corresponding effects on vibration indices. Also shown in Fig. 12 are data for the corresponding stiff baseline configuration. Again, the only difference between the three configurations in Fig. 12 is their spanwise mass distribution. The rotor design based exclusively on frequency placement criteria generates much higher vibratory forces than the one with a vibration index criteria. In fact, the frequency placement case has higher  $4P$  vibratory shears than the baseline case from which its design originates. The configuration order of the measured data matches that predicted by the analysis. In summary, criteria based exclusively on frequency placement does not provide rotor designs with optimum or even improved vibration characteristics.

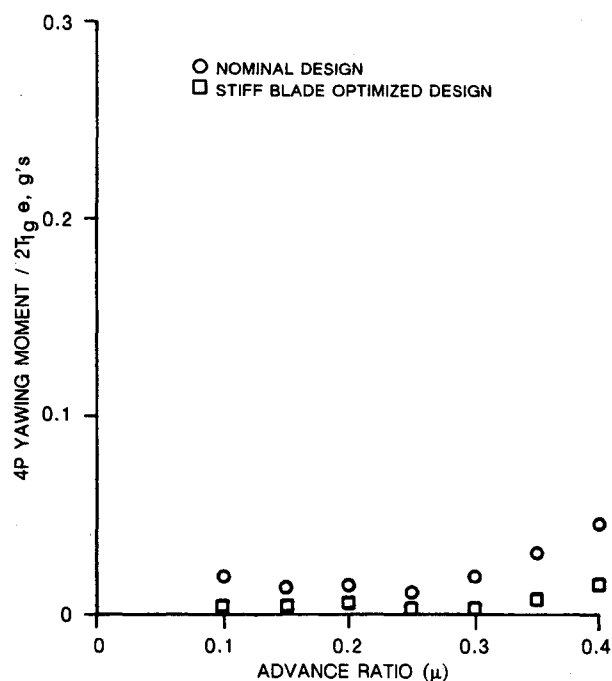
Figure 13 indicates the potential reductions in vibration levels that could be achieved by using both mass and structural stiffness as design parameters. As discussed previously, the nominal stiffness rotor configuration was chosen to approximate dynamic characteristics for a typical full-scale rotor. In optimization studies using both mass and stiffness variables, the analysis projected that optimization of this configuration to minimize vibratory response would require increasing structural bending-stiffness values to levels close to



a) Hub  $4P$  vertical shear



b) Total hub  $4P$  overturning moment



c) Hub  $4P$  yawing moment

Fig. 13 Attenuation of vibratory response by blade structural tailoring.

those of the stiff baseline blade. Thus, this potential gain is illustrated by optimizing the mass distribution of the stiff blade to achieve minimum vibration indices and comparing the measured results with those of the nominal blade. Comparisons of measured hub 4P vertical shear, 4P overturning moment, and 4P yawing (torque) moment are presented in Fig. 13 for 1g thrust. Although the overturning and yawing moments were not selected to be minimized by the optimization analysis, they are shown for completeness. From Fig. 13, the 4P vertical force for the optimized configuration is lower than that for the nominal configuration throughout the advance ratio range tested. At the highest advance ratio tested, the 4P vertical shear of the optimized design is 75% less than that of the nominal rotor. A comparable trend occurs for the 4P yawing moment with a reduction of 60% observed at the highest advance ratio. For the hub 4P overturning moment, comparable levels are seen at the moderate values of advance ratio, but up to 40% reductions from the nominal rotor levels are evident at the higher advance ratios.

### Conclusions

An automated design optimization analysis was developed to efficiently predict helicopter blade structural properties leading to improved dynamic behavior. Modal-based optimization criteria were defined for calculation by a coupled-mode eigenvalue analysis. Analytical studies were performed to project potential design benefits for various rotor dynamics problems and to evaluate techniques for improving the performance of the optimization analysis. Two experimental tests were also conducted to verify improved dynamic behavior predicted by the analysis for aeromechanical stability of a bearingless rotor and vibratory response of an articulated rotor. Direct comparisons were made in each test between the measured response for both dynamically scaled baseline and optimized model rotors. Results from this research program led to the following conclusions:

- 1) Parameter scaling by normalization provided significant improvement in optimizer performance.
- 2) MMFD and SQP were the most generally efficient and effective algorithms of the seven evaluated.
- 3) Min  $\beta$  and Min  $\Sigma\beta$  were viable alternatives to a sum-of-the-squares objective function formulation for problems having multiple objectives.
- 4) The optimization analysis efficiently predicted helicopter rotor designs having significantly improved stability and vibration characteristics through practical design changes.
- 5) Tests of existing and optimized bearingless rotor models confirmed the increase in structural damping predicted by the optimization analysis.
- 6) Frequency placement criteria alone was inadequate for minimizing rotor vibratory loads and may lead to increased vibratory response.
- 7) Minimizing either modal blade-root shears or vibration indices consistently resulted in significant reductions in measured peak 4P vibration levels at the hub relative to baseline designs. Measured reductions were greatest at high flight speeds, where baseline vibrations were highest.
- 8) Minimizing modal vibration indices was the most effective criteria considered for reducing rotor vibratory loads.

### Acknowledgments

The authors would like to acknowledge the assistance of the Aeromechanics Engineering Branch at Sikorsky Aircraft for

their contributions in design support, fabrication, and modification of much of the model hardware that was used in providing the experimental data in this paper. In particular, Ed Kiely, Chief of Experimental Aeromechanics, and Lee Kaplan, Model Laboratory Supervisor, were instrumental in coordinating these efforts and offering many helpful suggestions. The authors would also like to thank Gary Vanderplaats of VMA Engineering for helpful suggestions offered during the development of the blade design optimization analysis.

### References

- <sup>1</sup>Ashley, H., "On Making Things the Best—Aeronautical Uses of Optimization," *Journal of Aircraft*, Vol. 19, No. 1, 1982, pp. 5–28.
- <sup>2</sup>Miura, H., "Overview—Applications of Numerical Optimization Methods to Helicopter Design Problems," NASA CP-2327, April 1984, pp. 539–551.
- <sup>3</sup>Bennett, R. L., "Optimum Structural Design," *American Helicopter Society 38th Annual National Forum*, American Helicopter Society, Anaheim, CA, May 1982, pp. 398–407.
- <sup>4</sup>Peters, D. A., Ko, T., Korn, A., and Rossow, M. P., "Design of Helicopter Rotor Blades for Desired Placement of Natural Frequencies," *American Helicopter Society 39th Annual National Forum*, American Helicopter Society, Anaheim, CA, May 1983, pp. 674–689.
- <sup>5</sup>Friedmann, P. P., and Shanthakumaran, P., "Optimum Design of Rotor Blades for Vibration Reduction in Forward Flight," *Journal of the American Helicopter Society*, Vol. 29, No. 4, 1984, pp. 70–80.
- <sup>6</sup>Davis, M. W., "Optimization of Helicopter Rotor Blade Design for Minimum Vibration," NASA CP-2327, April 1984, pp. 609–625.
- <sup>7</sup>Yen, J. G., "Coupled Aeroelastic Hub Loads Reduction," *AHS/NAI International Seminar*, Nanjing, China, Nov. 1985, pp. D4-1–D4-9.
- <sup>8</sup>Davis, M. W., and Weller, W. H., "Application of Design Optimization Techniques to Rotor Dynamics Problems," *Journal of the American Helicopter Society*, Vol. 33, No. 3, 1988, pp. 42–50.
- <sup>9</sup>Celi, R., and Friedmann, P. P., "Structural Optimization with Aeroelastic Constraints of Rotor Blades with Straight and Swept Tips," AIAA Paper 88-2297, April 1988.
- <sup>10</sup>Lim, J. W., and Chopra, I., "Aeroelastic Optimization of a Helicopter Rotor," *Journal of American Helicopter Society*, Vol. 34, No. 1, 1989, pp. 52–62.
- <sup>11</sup>Weller, W. H., and Davis, M. W., "Wind Tunnel Tests of Helicopter Blade Designs Optimized for Minimum Vibration," *Journal of the American Helicopter Society*, Vol. 34, No. 3, 1989, pp. 40–50.
- <sup>12</sup>Vanderplaats, G. N., Sugimoto, H., and Sprague, C. M., "ADS-1: A New General-Purpose Optimization Program," *AIAA Journal*, Vol. 22, No. 10, 1984, pp. 1458–1459.
- <sup>13</sup>Vanderplaats, G. N., "ADS—A Fortran Program for Automated Design Synthesis (Version 1.00)," Naval Postgraduate School, Monterey, CA, May 1984.
- <sup>14</sup>Weller, W. H., and Mineck, R. E., "An Improved Computational Procedure for Determining Helicopter Rotor Blade Natural Modes," NASA TM-78670, Aug. 1978.
- <sup>15</sup>Fox, R. L., *Optimization Methods for Engineering Design*, Addison-Wesley, Reading, MA, 1973.
- <sup>16</sup>Reklaitis, G. V., Ravindran, A., and Ragsdell, K. M., *Engineering Optimization*, John Wiley and Sons, New York, 1983.
- <sup>17</sup>Vanderplaats, G. N., *Numerical Optimization Techniques for Engineering Design*, McGraw-Hill, New York, 1984.
- <sup>18</sup>Vanderplaats, G. N., "An Efficient Feasible Directions Algorithm for Design Synthesis," *AIAA Journal*, Vol. 22, No. 11, 1984, pp. 1633–1640.
- <sup>19</sup>Weller, W. H., and Peterson, R., "Inplane Stability Characteristics for an Advanced Bearingless Main Rotor Model," *Journal of the American Helicopter Society*, Vol. 29, No. 3, 1984, pp. 45–53.
- <sup>20</sup>Blackwell, R. H., "Blade Design for Reduced Helicopter Vibration," *Journal of the American Helicopter Society*, Vol. 28, No. 3, 1983, pp. 33–41.